


Theory of Gravitons in Spiral and Dwarf Galaxy Rotation Curves

Firmin J. Oliveira 

East Asian Observatory/James Clerk Maxwell Submillimetre Telescope, 660 N. A'ohoku Place, Hilo, Hawaii, USA
Email: firmjay@hotmail.com

How to cite this paper: Oliveira, F.J. (2022) Theory of Gravitons in Spiral and Dwarf Galaxy Rotation Curves. *Journal of High Energy Physics, Gravitation and Cosmology*, 8, 810-834.
<https://doi.org/10.4236/jhepgc.2022.83055>

Received: June 14, 2022

Accepted: July 26, 2022

Published: July 29, 2022

Copyright © 2022 by author(s) and Scientific Research Publishing Inc. This work is licensed under the Creative Commons Attribution International License (CC BY 4.0).

<http://creativecommons.org/licenses/by/4.0/>



Open Access

Abstract

We hypothesize that gravitons contribute significantly to the process that flattens galaxy rotation curves. Gravitons travelling against a gravitational field experience an energy loss due to gravitational redshift identical to the effect on light. This energy loss requires an increased rotational velocity to stabilize a galaxy. We will show that this approach successfully explains the rotational properties of spiral and dwarf galaxies.

Keywords

Gravitons, Spiral Galaxies, Galaxy Dynamics, Newtonian Mechanics, Hubble's Law, Baryonic Tully-Fisher Relation

1. Introduction

For nearly a century scientists have been searching for the cause of the larger-than-expected rotational velocities of galaxies in a cluster [1] and the unexpected speedy rotation of stars in flat, spiral galaxies [2]. Many investigators have suggested that extra mass is required, up to an order of magnitude more, than what is calculated assuming galactic mass is proportional to luminosity. These observations have been attributed to dark matter particles; these neither absorb nor emit light and only interact with other matter forms by gravity. The standard model of particle physics does not offer a particle with suitable attributes to satisfy all the requirements of dark matter particle(s). Many attempts to directly observe such particles have failed [3].

We have previously suggested that the graviton, the hypothetical agent of the gravitational field, may help explain much of the stellar rotational velocities observed for stars in spiral and dwarf galaxies [4] [5]. Since the rotational speeds involved are small compared with the speed of light, we use only Newtonian physics to present our arguments. We account for galaxy rotational speeds via

graviton energy loss without referring to dark matter. We conclude that there is no requirement for a halo distribution of dark matter about spiral and dwarf spiral galaxies. Furthermore, we show how the Hubble law and the baryonic Tully-Fisher relation (BTFR) can be derived from the graviton energy loss concept.

The enigma of dark matter in galaxies can also be addressed in the framework of the Extended Theories of Gravity [6], although here we do not describe these theories in any detail.

2. Theory of Gravitons

We treat gravitons as relativistic bosonic particles which travel at constant velocity, c , in a vacuum, where c is the speed of light. Gravitons travelling in a gravitational field are considered a source of masses M and m , and are modelled by the equivalence principle in an accelerating system. In such a system, over a short time period $\delta t = \delta r/c$, gravitons should experience an average energy loss of $\delta \Xi_g$ due to motion in that field, where the acceleration a at a point r in the field is given by $a = -GM/r^2$. The energy loss during this period is expressed differentially as,

$$\delta \Xi_g = -\left(m_g c^2\right) \frac{\delta u}{c} = \left(m_g c\right) a \delta t = -\left(\frac{GMm_g}{r^2}\right) \delta r, \tag{1}$$

where $m_g = m/n$ is the average relativistic graviton mass, n is the average number of gravitons, m is the test mass, δu is the change in velocity of the system observed from an inertial reference frame, G is Newton’s gravitational constant, M is the mass of the field source, r is the distance between the center of the source and the location of the moving gravitons, δt is the short travel time of the gravitons over distance δr . The energy change is a loss (negative) because δu is in the same direction as the graviton motions. For an inertial observer moving at some velocity u in the direction of δu , the energy of the graviton is redshifted.

Now, viewing the system as a whole, consider gravitons travelling in a gravitational field where the field is equivalent to an accelerating system. We can assume that the total graviton energy for the system of two masses M and m at distance r between centers, by Newton’s law of gravitation, is given by

$$\Xi = \frac{GMm}{r}, \tag{2}$$

where $m = nm_g$ is the total graviton mass representing the test mass m , and where m_g is the average graviton relativistic mass and n is the number of gravitons. The graviton energy decrease $\delta \xi$ due to the free-fall in the gravitational field of mass M , when viewed from an inertial system, is expressed by

$$\delta \xi = \Xi \frac{\delta u}{c} = -\left(\frac{GMnm_g}{r}\right) \frac{\delta u}{c}, \tag{3}$$

where δu is the velocity increase in the accelerated reference frame, which is equivalent to the acceleration caused by the gravitational field of mass M at the

position r . Multiplying (1) by the number of gravitons n and equating the result to (3) yields

$$n\delta\Xi_g = -\left(\frac{GMnm_g}{r^2}\right)\delta r = \delta\zeta = -\left(\frac{GMnm_g}{r}\right)\frac{\delta u}{c}, \tag{4}$$

which simplifies to

$$\frac{\delta r}{r} = \frac{\delta u}{c}. \tag{5}$$

Integrating (5) from r_1 to r , where

$$r_1 = r/\exp(rH_0/c), \tag{6}$$

and where $r \leq c/H_0$, where H_0 is defined as the local Hubble's constant, we obtain

$$\int_{r_1}^r \frac{dr}{r} = \ln\left(\frac{r}{r_1}\right) = \frac{H_0 r}{c} = \int_0^u \frac{\delta u}{c} = \frac{u}{c}. \tag{7}$$

Here we use the fact that $\ln(r/r_1) = \ln(r/\exp(rH_0/c)) = rH_0/c$. Since $\exp(rH_0/c) \geq 1$ and therefore $r_1 \leq r$, we simplify (7) to give us,

$$u = H_0 r. \tag{8}$$

We recognise this as Hubble's law [7], where in this case u is the instantaneous free fall velocity of a particle in the source gravitational field and r is the distance of the graviton from the source. To be clear, in (8), u is the velocity of free fall relative to the equivalent accelerating reference frame, and not the velocity of the mass m orbiting mass M .

Differentiating (8) with respect to time t we obtain the acceleration a_g as

$$a_g = \frac{du}{dt} = H_0 \frac{dr}{dt} = cH_0, \tag{9}$$

where the graviton velocity is $dr/dt = c$. The acceleration a_g is not the acceleration due to the source mass M , but is instead the rate of change of the free fall velocity field u relative to an inertial reference frame. The acceleration a_g acting over a distance r is a potential function $U(r)$ which we term the *graviton induced potential*, defined by integrating (9) over distance r ,

$$U(r) = -\int_0^r cH_0 dr = -cH_0 r, \tag{10}$$

where we introduce the minus sign so that the force $-m dU(r)/dr = mcH_0$ is in the positive r direction as given by (9).

Integrating (1) up to radial distance r we obtain the average energy change per graviton $\Delta\Xi_g$, given by

$$\Delta\Xi_g = -\int_0^r (m_g c^2) \frac{du}{c} = -\int_0^r m_g \left(\frac{GM}{r^2}\right) dr. \tag{11}$$

Equation (11) describes the gravitational redshift of the energy of the average graviton as it travels from a lower, more negative potential to a position r of higher, less negative potential and is consistent with energy conservation.

The physics of individual gravitons is a means to describe how an energy loss

comes about due to the free falling of energy in a gravitational field. After we sum up all the energy losses due to the gravitons in free fall in the field, we obtain the energy loss of the field itself. In other words, in the form of gravitons, the relativistic gravitational field energy travels at speed c between the non-relativistic masses M and m and there occurs an energy loss to the field. It may be that the effect due to the gravitons is detectable but the gravitons themselves are not [8], similar to the role of quarks in particle physics.

2.1. Gravitons in Galaxies

Now, consider the energy for a galaxy of mass M interior of a small mass m in a circular orbit of radius r . The gravitons traversing the distance at lightspeed from the interior mass to the orbiting mass will experience a decrease in energy as described by (11), $\Delta \Xi = n \Delta \Xi_g$, where n is the number of gravitons. Taking the energy loss of the gravitons into account, the total orbital energy of the orbiting mass m is given by

$$\frac{1}{2}mv^2 - \frac{GMm}{r} + K_g n \Delta \Xi_g = E, \tag{12}$$

where v is the rotational velocity of the orbiting mass, K_g is a coupling coefficient, which we assume is constant for each galaxy, and the total energy $E = -GM/2r$. Expanding $\Delta \Xi_g$ using (11), with $m = nm_g$, multiplying by $2/m$ and moving all terms except v^2 to the right hand side, we obtain the expression for the orbital velocity,

$$v^2 = \frac{GM(r)}{r} + 2K_g \int_0^r \left(\frac{GM(r)}{r^2} \right) dr. \tag{13}$$

As an approximation, we model the mass distribution of a spiral galaxy by a spherically symmetric distribution $\rho(r)$, even though a mass density distribution consisting of a spherically symmetric central bulge surrounded by an axially symmetric thin disk would be more realistic. Then the mass $M(r)$ of the galaxy within the radial distance r from the galaxy center is given by,

$$M(r) = \int_0^r 4\pi\rho(r)r^2 dr. \tag{14}$$

In subsequent sections we will apply our theory to the rotation curves of some typical spiral and dwarf spiral galaxies. The quality of the fits to the real galaxy data will justify the approximate mass distribution we have assumed.

2.2. Coupling Coefficient K_g

Under our assumption that the coupling coefficient is constant for each galaxy, (13) can be solved for K_g at the galaxy edge, where $r = r_f$ and $v = v_f$, giving

$$K_g = \frac{v_f^2 - \frac{GM(r_f)}{r_f}}{2 \int_0^{r_f} \left(\frac{GM(r)}{r^2} \right) dr}, \tag{15}$$

where $M(r_f) = M_b$ is the total baryonic mass in the galaxy. By Newton’s gravitational law, at the galaxy edge, the final velocity v_f is related to the total mass M_g contained within the radial distance r_f by,

$$v_f^2 = \frac{GM_g}{r_f} = \frac{G(M_b + M_d)}{r_f}, \tag{16}$$

where $M_g = M_b + M_d$, where M_d is the total apparent mass due to the graviton energy loss, the mass of the so called “dark matter”. The total apparent dark matter in a galaxy is given at the galaxy edge by,

$$M_{d\,obs} = \frac{v_f^2 r_f}{G} - M_b. \tag{17}$$

Using the results from analysing galaxy rotational data we can estimate the dark matter by (17) as $M_{d\,b}$ and substituting that and (16) into (15) we arrive at a formula for estimating K_g as

$$K_g = \frac{M_{d\,obs}}{2r_f \int_0^{r_f} \left(\frac{M(r)}{r^2} \right) dr}. \tag{18}$$

3. The Baryonic Tully-Fisher Relation

The BTFR [9] [10] is an empirical relation expressed in the form,

$$M_b = Av_b^4, \tag{19}$$

where M_b is the total baryonic mass of the galaxy, v_b the velocity of the flat portion of the galaxy velocity rotation curve and A is a constant. We can derive this relation by using the differential of (10) in the form

$$-v\,dv = -cH_0\,dr. \tag{20}$$

Then modulating the Newtonian circular orbit equation $v^2 = GM/r$ with (20), dropping the minus sign from both sides, and integrating the result yields

$$\int_{v_a}^{v_b} (v^2) v\,dv = \int_{r_a}^{r_b} \left(\frac{GM}{r} \right) cH_0\,dr, \tag{21}$$

where v_a is the initial velocity at radial distance r_a , v_b is the velocity at the flat portion of the rotation curve beginning at radial distance r_b . It is assumed that the points (r_a, v_a) and (r_b, v_b) are in close proximity, where $r_a < r_b$ and $v_a < v_b$ and $M \approx M_b$, the total baryonic mass of the system. Solving the integrals (21) and putting this into the form of the BTFR we have

$$M_b = \left(\frac{1 - (v_a/v_b)^4}{4 \ln(r_b/r_a)} \right) \left(\frac{1}{cH_0G} \right) v_b^4 = \left(\frac{1}{\alpha cH_0G} \right) v_b^4 \tag{22}$$

where $\alpha = 4 \ln(r_b/r_a) / (1 - (v_a/v_b)^4)$. Assuming $r_b = r_a + \Delta r$, where $\Delta r \ll r_a$, and $v_b = v_a + \Delta v$, where $\Delta v \ll v_a$, we can better understand what α is by taking the approximation,

$$\alpha \approx \left(\frac{v_a}{r_a} \right) \left(\frac{\Delta r}{\Delta v} \right) = \left(\frac{mv_a^2}{r_a} \Delta r \right) \left(1/\Delta \left(\frac{mv_a^2}{2} \right) \right) = \frac{\Delta E}{\Delta KE}, \tag{23}$$

where ΔE is the change in total energy and ΔKE is the change in kinetic energy. Since the value of the BTFR coefficient A in (19) is an average of many observations of spiral galaxy rotation curve data, we assume that α is an average related to these observations. From (19) and (22), with

$H_0 = 72.1 \text{ km} \cdot \text{s}^{-1} \cdot \text{Mpc}^{-1}$ and $A = 50 M_{\odot} \cdot \text{s}^4 \cdot \text{km}^{-4}$, we can estimate a value for this parameter,

$$\alpha = \left(\frac{1}{AcH_0G} \right) \left(\frac{10^{12}}{M_{sol}} \right) = 0.215. \quad (24)$$

We see that at the transition from Newtonian to non-Newtonian motion, the change in kinetic energy is about 4.65 times the change in total energy. The value given in (24) is an average taken from a large sample of galaxies, but in general, α will have a value peculiar to each galaxy.

4. Results for SPARC Mass Densities

To test the viability of the graviton model for spiral galaxies we will use the velocities from Spitzer Photometry and Accurate Rotation Curves (SPARC) data base [11] [12], derived from near-infrared (NIR) surface photometry at $3.6\mu\text{m}$. For comparison of galaxies for which we used simulated mass densities, we selected the galaxies NGC 2403, NGC 2841, NGC 2903, NGC 3198, NGC 6503, NGC 7331, DDO 154 and NGC 2915. In addition we selected also UGCA 442, UGCA 444, UGC 02953, UGC 05953, IC 2574 and IC 4202. From the photometric data which has been reduced to the equivalent velocities for the galaxy bulge, disk and gas mass content, we approximate the baryonic mass as due to a spherically symmetric distribution, which is given by the Newtonian relation for the velocity to mass contained within the radius r from the galaxy center, expressed by

$$M_b(r) = \left(\frac{r}{G} \right) \left(|v_{gas}(r)|v_{gas}(r) + \Upsilon_{disk}(r)|v_{disk}(r)|v_{disk}(r) + \Upsilon_{bul}(r)|v_{bul}(r)|v_{bul}(r) \right), \quad (25)$$

where $r = r_i$, $i = 1, 2, \dots, N$, $N > 1$, N the number of radial distances observed, and the absolute values of the velocities are needed because they can sometimes be negative (Ref. [13]: p. 5). The velocities for the disk and gas from Table 2 of [11] are taken with $\Upsilon_* = 1$. In our Table 2, Υ_{disk} and Υ_{bul} are the M_{\odot}/L_{\odot} used in (25) to make the fits. Approximating the mass density assuming a spherically symmetric distribution, at distance r using (25) the mass density is then given by,

$$\rho(r) = \frac{3M_b(r)}{4\pi r^3}. \quad (26)$$

Using the SPARC results for the mass at r in terms of the gas, disk and bulge velocities, where the mass internal to r is given by $M_b(r)$ of (25), the predicted velocity (13) is expressed in the form,

$$v^2(r_n) = \frac{GM_b(r_n)}{r_n} + 2K_g \sum_{j=1}^n \left(\int_{r_{j-(j>1)}}^{r_{j+(j<2)}} \left(\frac{GM_b(r)}{r^2} \right) dr \right), \quad (27)$$

where $n = 1, 2, \dots, N$, $N > 1$. Regarding K_g from (17), (18) and (27) with $r = r_f$, the final radial distance and $v_{obsf} = v_f$, the final galaxy rotation velocity,

$$K_g = \frac{M_{dobs}}{2r_f \int_0^{r_f} \left(\frac{M_b(r)}{r^2} \right) dr} = \frac{\left(\frac{v_{obsf}^2}{G} \right) r_f - M_b}{2r_f \sum_{j=1}^N \left(\int_{r_{j-(j>1)}}^{r_{j+(j<2)}} \left(\frac{M_b(r_j)}{r_j^2} \right) dr \right)}. \quad (28)$$

In order to fit the mass to light ratio for the disk component while keeping the bulge component fixed, or vis-a-versa, we apply the relationship for a new iteration of the δY_x , where $x = dsk$ or $x = bul$,

$$\delta Y_x(r_k) = \frac{v_{obs}^2(r_k)}{v^2(r_k)}, \quad (29)$$

where $v_{obs}(r_k)$ is the observed velocity at radial distance r_k and $v(r_k)$ is the predicted velocity (13) using the graviton model. Then iterating to get a new $Y_x(r_k)$ is obtained by,

$$Y_x(r_k) = \delta Y_x(r_k) (Y_x(r_k)). \quad (30)$$

We adhered to two constraints while fitting to the SPARC galaxy data: first, get the derived galaxy baryonic mass from the fit to nearly equal the BTFR predicted mass using the final rotation velocity for the galaxy, which may not equal the flat velocity which the BTFR requires; and second, obtain good fits to the velocity $v_{obs}(r_k)$ at each radial distance r_k by minimizing the mean absolute error MAE between $v(r_k)$ and $v_{obs}(r_k)$ while iterating $Y_{dsk}(r_k)$ for the disk and, when available, $Y_{bul}(r_k)$ for the bulge, as specified by (27)-(30). Eventually we found out that by initially using equal constant Y_* for the disk and bulge M/L values until the derived galaxy mass closely approximated the BTFR mass value, the derived mass remained fixed to this value as we executed the iteration process to obtain Y_* at each r_k . There has to be a simple explanation for this behavior. **Table 1** lists for each galaxy the baryonic mass M_b determined by the velocity profiles used in (25), the mean data rotation velocity error V_{err} the mean absolute fitted error MAE and the coupling coefficient K_g .

Table 2 lists the ranges for disk Y_{dsk} and bulge Y_{bul} mass to light ratios which were used in making each galaxy fit. Also listed in the table are minimum and maximum Y_{dsk} taken from Table 4 and Table 5 of [13] for comparison. In general our disk mass to light ratios are compliant with the maximum Y_{dsk} values, though DDO 154 has excessive mass to light in our fit. A good reference for fits to SPARC data can also be found in [14], especially for spiral galaxy NGC 2841, where from **Table 2** we have the range of Y_{dsk} between $0.6 - 1.6 M_\odot/L_\odot$ and Y_{bul} between $0.8 - 1.6 M_\odot/L_\odot$, each of which is of the same order of magnitude as the fitted values $Y_{disk} = 0.81 \pm 0.05 M_\odot/L_\odot$ and $Y_{bul} = 0.93 \pm 0.05 M_\odot/L_\odot$, respectively, from **Figure 1** of [14].

Table 1. Results of fits to SPARC galaxy data using the graviton model (27) with mass and density from (25) and (26). The V_{err} are the means of the errors of the reported stellar velocities. MAE errors are the average absolute error for the fits. The coefficient K_g is the value obtained from (28) for each fit.

Galaxy	M_b ($M_\odot \times 10^{10}$)	† M_b BTFR ($M_\odot \times 10^{10}$)	V_{err} ($\text{km}\cdot\text{s}^{-1}$)	MAE ($\text{km}\cdot\text{s}^{-1}$)	K_g
NGC 2403	1.612	1.612	2.421	0.652	0.422
NGC 2841	37.353	37.356	7.67	1.168	0.189
NGC 2903	5.249	5.249	4.029	0.846	0.140
NGC 3198	2.462	2.464	5.043	0.613	0.427
NGC 6503	0.8744	0.8745	2.355	0.444	0.305
NGC 7331	16.071	16.043	5.139	0.640	0.181
DDO 154	0.04985	‡ 0.02143	0.625	0.149	0.706
NGC 2915	0.2875	0.2799	8.064	1.247	0.610
UGCA 442	0.1160	‡ 0.05095	2.004	0.429	0.621
UGCA 444	0.03177	‡ 0.01076	3.909	0.681	0.785
UGC 02953	27.378	27.368	6.851	0.638	0.102
UGC 05053	11.297	11.293	5.951	0.745	0.086
IC 2574	0.4489	‡ 0.1038	3.241	0.411	0.880
IC 4202	18.608	18.611	7.368	0.257	0.177

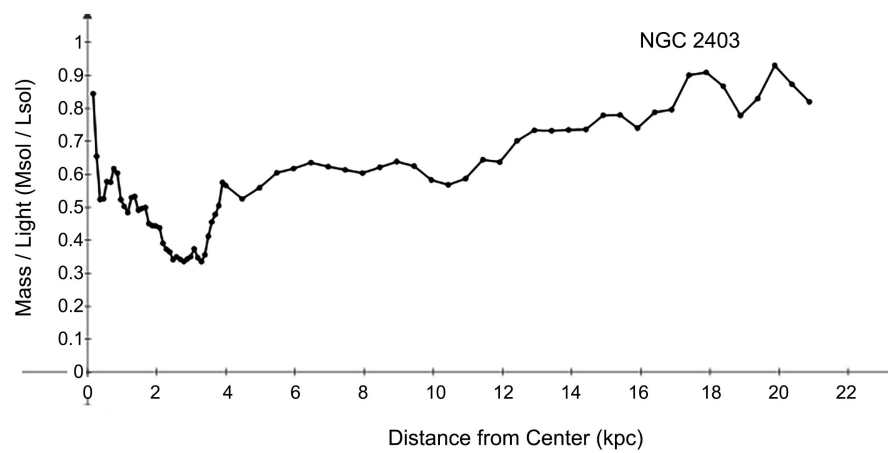
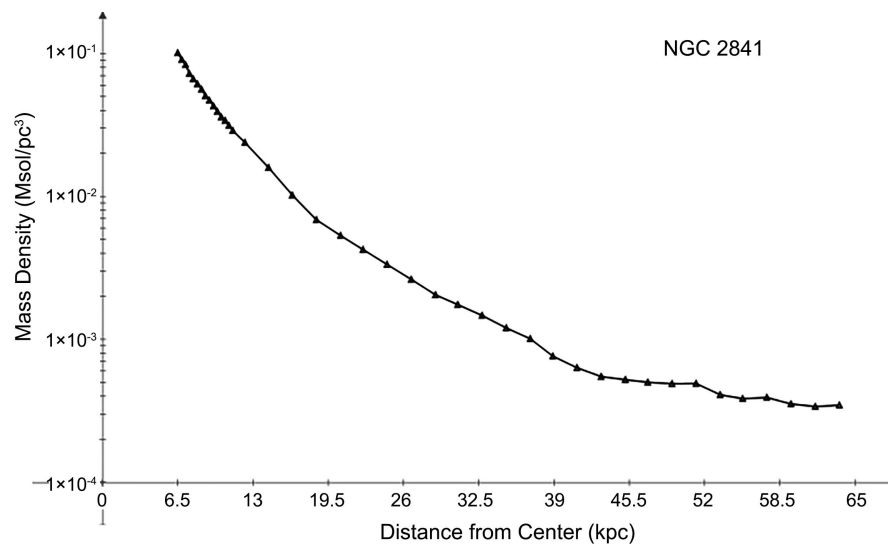
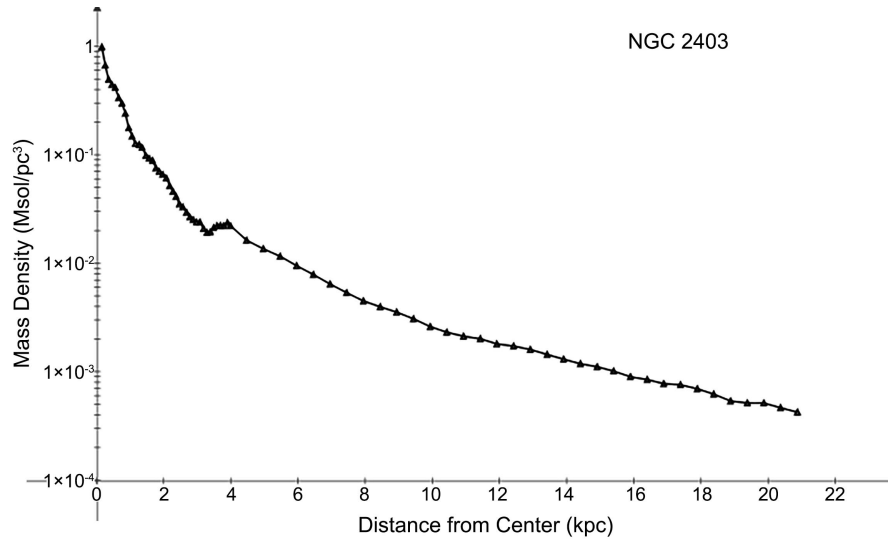
† Using final velocity as flat velocity. ‡ Rotation curve does not flatten.

Table 2. Results of fits to SPARC galaxy data using the graviton model (27). The columns for Υ_{dsk} and Υ_{bul} are the ranges for the disk and bulge mass to light ratios determined by modeling the rotation velocity curve.

Galaxy	Υ_{dsk}	Υ_{bul}	† min Υ_{dsk}	† max Υ_{dsk}
NGC 2403	0.336 - 0.930	0	1.3	1.8
NGC 2841	0.621 - 1.594	0.830 - 1.594	2.0	5.1
NGC 2903	0.043 - 0.581	0	1.7	2.9
NGC 3198	0.030 - 0.711	0	1.4	3.5
NGC 6503	0.369 - 0.905	0	1.6	1.7
NGC 7331	0.321 - 0.552	0.192 - 0.553	n	5.8
DDO 154	0.640 - 9.317	0	1.1	1.2
NGC 2915	0.049 - 3.591	0	n	n
UGCA 442	1.383 - 4.828	0	n	n
UGCA 444	3.876 - 12.0	0	n	n
UGC 02953	0.456 - 0.987	0.203 - 7.503	n	n
UGC 05053	0.314 - 0.633	0.327 - 2.211	n	n
IC 2574	0.545 - 2.154	0	n	n
IC 4202	0.602 - 0.810	0.039 - 0.956	n	n

0 in the Υ_{bul} column means the bulge velocity is zero in the data. † Min and max Υ_{dsk} values for high surface mass galaxies from [13]. n means the result is not available.

For dwarf galaxy IC 2574, our range for Υ_{disk} is $0.55 - 2.15 M_{\odot}/L_{\odot}$, which is about $20\times$ larger than the $\Upsilon_{disk} = 0.07 \pm 0.01 M_{\odot}/L_{\odot}$ obtained in the fit shown in **Figure A1** of [14], although our Υ_{disk} range is physically reasonable.



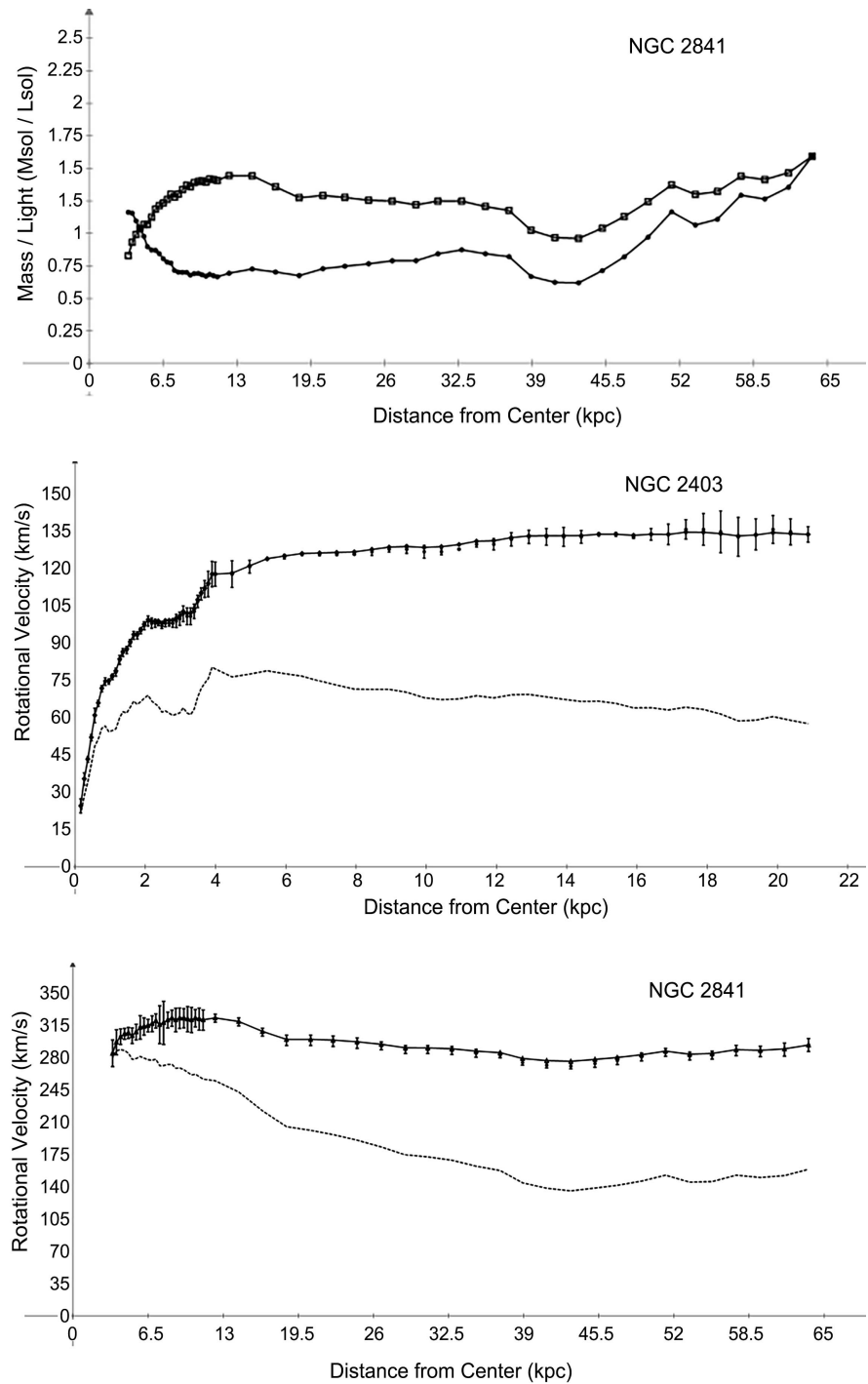


Figure 1. Fits with SPARC data, the mass density derived from (26) with velocity profiles for gas, disk and bulge. For mass to light curves, Υ_{disk} is the solid line and filled circles, Υ_{bul} is the solid line and open squares. For rotation velocity curves, the solid line is the minimised fit to the data with the graviton model (27) and the dashed line is the Newtonian velocity. Upper left: NGC 2403 mass density. Middle left: Mass to light ratio. Lower left: The model velocity vs. radial distance from the galactic center and the Newtonian velocity. Upper right: NGC 2841 mass density. Middle right: Mass to light ratio. Lower right: The model velocity vs. radial distance from the galactic center and the Newtonian velocity.

For each plot of the galaxy rotation velocity, the Newtonian velocity curve is also displayed. Plots for the results of the SPARC galaxies can be found in **Figure 1** in the main body of the paper and in Appendix A for **Figures A1-A6**.

SPARC Galaxies DDO 154 and NGC 2915

Two galaxies that have been difficult to understand in terms of missing mass are dwarf spiral DDO 154 and spiral NGC 2915. We did a deeper analysis to fitting the rotation curve by the iterative process given by (29) and (30). **Figure A3** shows the results for the fits. The upper curves show the mass density, the middle curves display the M/L ratios and the lower plots show the observed and predicted rotation velocities. For DDO 154 we obtained with the graviton model a total baryonic mass of $M_{bary} = 4.99 \times 10^8 M_{\odot}$, which is less than twice the detected luminous mass [15] of $M_* + M_{HI+He} = 3.65 \times 10^8 M_{\odot}$. Significantly, it is only one-sixth of the estimated dark plus luminous matter of $M_{dark+lum} = 3.1 \times 10^9 M_{\odot}$. However, our fitted disk mass to light ratios have a range of $0.64 M_{\odot}/L_{\odot} \leq \Upsilon_{disk} \leq 9.3 M_{\odot}/L_{\odot}$, which is excessive compared to the published value of about $\Upsilon_{disk} \approx 2 M_{\odot}/L_{\odot}$.

For NGC 2915 we obtained a total baryonic mass of $M_{bary} = 2.88 \times 10^9 M_{\odot}$, where the stellar mass and luminous HI mass [16] [17] $M_{HI} + M_* = 1.06 \times 10^9 M_{\odot}$. This compares with the total dynamical mass $M_T = 21 \times 10^9 M_{\odot}$ which is 7×the total baryonic mass derived by the graviton model.

5. Conclusions

We have presented the graviton model to describe the rotational characteristics of spiral and dwarf spiral galaxies. We used velocity data from the SPARC data base derived from NIR photometry. We included seven of the galaxies from the NGC catalog and one from the DDO catalog and an additional six galaxies from the UGC and IC catalogs. For the sample of galaxies, we considered, we think our graviton theory does quite well at explaining the greater than expected galaxy rotational velocities in the SPARC data with only the baryonic mass derived from the gas, disk and bulge velocity data and fitted Υ_* ratios and the mass agreeing with the BTFR predictions for galaxies whose rotation curves flattened. The algorithm we have described can be readily automated.

Finally, using the graviton redshift model we derived a Hubble law for galaxies and also showed how the interaction of the gravitational field with the induced graviton field can explain the baryonic Tully-Fisher relation.

Acknowledgements

Thanks to Mike Smith for support and inspiration. Thanks also to F. Lelli, S. S. McGaugh and J. M. Schombert for making the SPARC data available online.

Conflicts of Interest

The author declares no conflicts of interest regarding the publication of this paper.

References

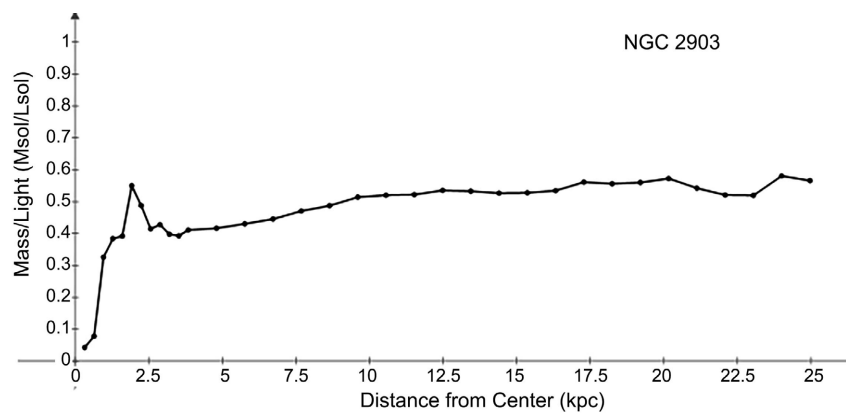
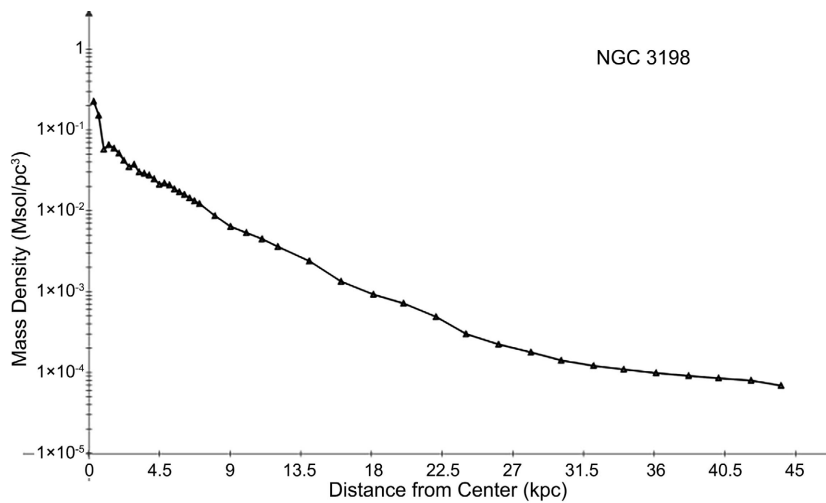
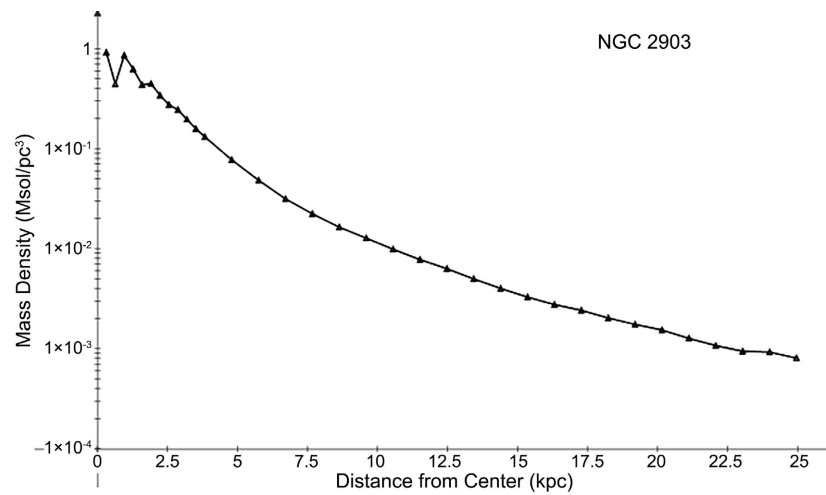
- [1] Zwicky, F. (1937) On the Masses of Nebulae and of Clusters of Nebulae. *The Astrophysical Journal*, **86**, 217-246. <https://doi.org/10.1086/143864>
- [2] Rubin, V.C. and Ford Jr., W.K. (1970) Rotation of the Andromeda Nebula from a Spectroscopic Survey of Emission Regions. *The Astrophysical Journal*, **159**, 379-403. <https://doi.org/10.1086/150317>
- [3] Luminet, J.P. (2020) The Dark Matter Enigma. *Inference*, **5**, 6 p. <https://inference-review.com/article/the-dark-matter-enigma>
<https://doi.org/10.37282/991819.20.32>
- [4] Oliveira, F.J. (2021) The Principle of Equivalence: Periastron Precession, Light Deflection, Binary Star Decay, Graviton Temperature, Dark Matter, Dark Energy and Galaxy Rotation Curves. *Journal of High Energy Physics, Gravitation and Cosmology*, **7**, 661-679. <https://doi.org/10.4236/jhepgc.2021.72038>
- [5] Oliveira, F. and Smith, M.L. (2022) Dark Matter in Spiral Galaxies as the Gravitational Redshift of Gravitons. In: Smith, M.L., Ed., *Dark Matter—Recent Observations and Theoretical Advances*, IntechOpen, London. <https://doi.org/10.5772/intechopen.101130>
- [6] Corda, C. (2009) Interferometric Detection of Gravitational Waves: the Definitive Test for General Relativity. *International Journal of Modern Physics D*, **18**, 2275-2282. <https://doi.org/10.1142/S0218271809015904>
- [7] Hubble, E. (1929) A Relation between Distance and Radial Velocity among Extra-Galactic Nebulae. *Proceedings of the National Academy of Sciences of the United States of America*, **15**, 169-173. <https://doi.org/10.1073/pnas.15.3.168>
- [8] Dyson, F. (2013) Is a Graviton Detectable? *International Journal of Modern Physics A*, **28**, Article ID: 1330041. <https://doi.org/10.1142/S0217751X1330041X>
- [9] McGaugh, S.S. (2005) The Baryonic Tully-Fisher Relation of Galaxies with Extended Rotation Curves and the Stellar Mass of Rotating Galaxies. *The Astrophysical Journal*, **632**, 859-871. <https://doi.org/10.1086/432968>
- [10] Lelli, F., McGaugh, S.S. and Schombert, J.M. (2016) The Small Scatter of the Baryonic Tully-Fisher Relation. *The Astrophysical Journal Letters*, **816**, L14-L19. <https://doi.org/10.3847/2041-8205/816/1/L14>
- [11] <http://astroweb.cwru.edu/SPARC/>
- [12] Lelli, F., McGaugh, S.S. and Schombert, J.M. (2016) SPARC: Mass Models for 175 Disk Galaxies with Spitzer Photometry and Accurate Rotation Curves. *The Astrophysical Journal*, **152**, 157-170. <https://doi.org/10.3847/0004-6256/152/6/157>
- [13] De Blok, W.J.G. and McGaugh, S.S. (1997) The Dark and Visible Matter Content of Low Surface Brightness Disk Galaxies. *Monthly Notices of the Royal Astronomical Society*, **290**, 533-552. <https://doi.org/10.1093/mnras/290.3.533>
- [14] Li, P., Lelli, F., McGaugh, S. S. and Schombert, J. M. (2018) Fitting the Radial Acceleration Relation to Individual SPARC Galaxies. *Astronomy & Astrophysics*, **615**, Article No. A3. <https://doi.org/10.1051/0004-6361/201732547>
- [15] Carignan, C. and Purton, C. (1998) The “Total” Mass of DDO 154. *The Astrophysical Journal*, **506**, 125-134. <https://doi.org/10.1086/306227>
- [16] Meurer, G.R., Carignan, C., Beaulieu, S.F. and Freeman, K.C. (1996) NGC 2915. II. A Dark Spiral Galaxy with a Blue Compact Dwarf Core. *Astronomical Journal*, **111**, 1551-1575. <https://doi.org/10.1086/117895>
- [17] Meurer, G.R., Blakeslee, J.P., Sinanni, M., Ford, H.C., Illingworth, G.D., Benitez, N.,

et al. (2003) The Discovery of Globular Clusters in the Protospiral Galaxy NGC 2915: Implications for Hierarchical Galaxy Evolution. *The Astrophysical Journal*, **599**, L83-L86. <https://doi.org/10.1086/381317>

Appendices

Appendix A: More Rotation Curve Fits Using SPARC Mass Density Profiles

Curve fits to galaxy data using SPARC mass densities from (25) and (26) with velocity profiles for gas, disk and bulge. The mass-to-light curves are generated using (29) and (30). The rotation curves are generated from (27). Note: the caption description for each figure is out of order.



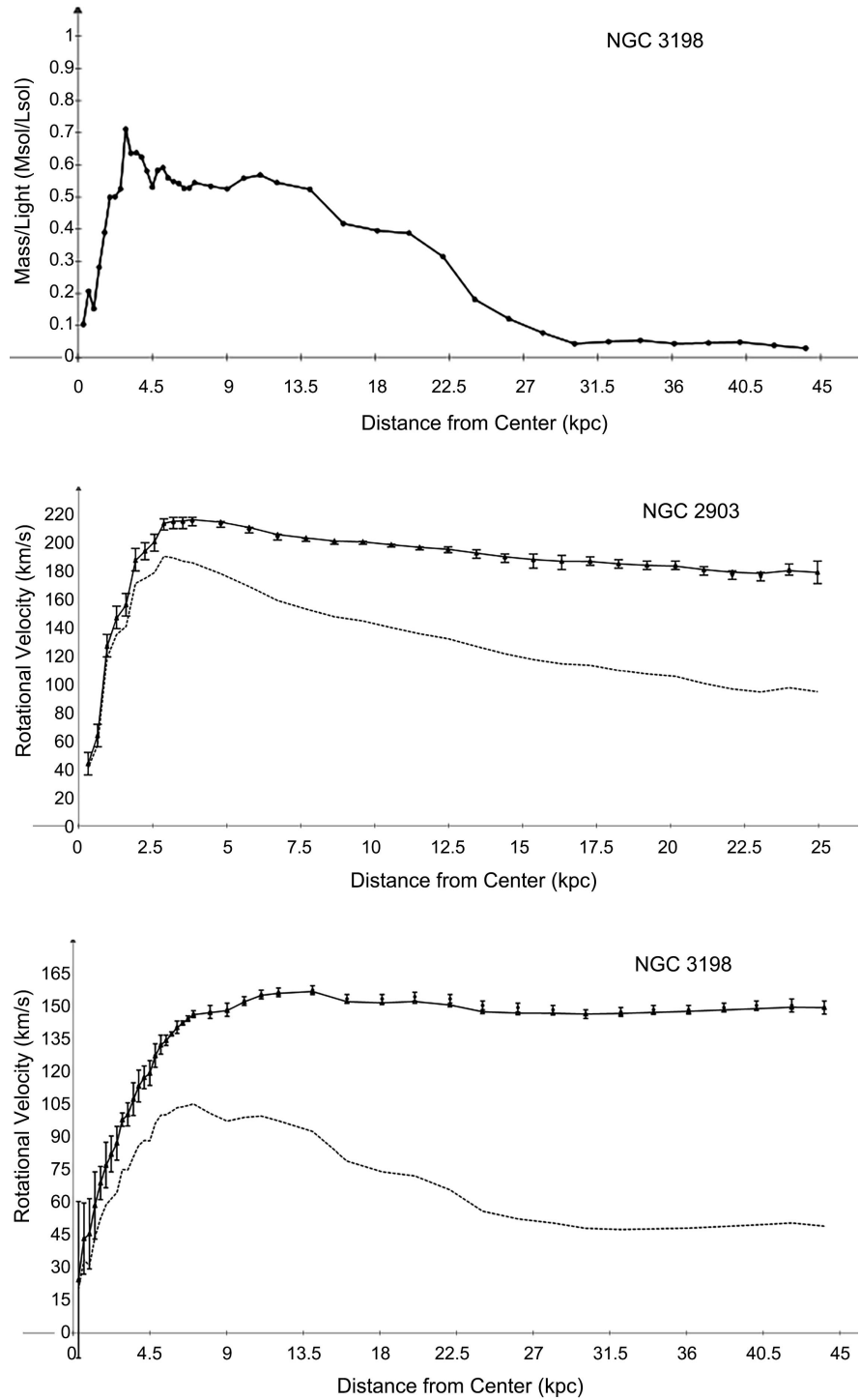
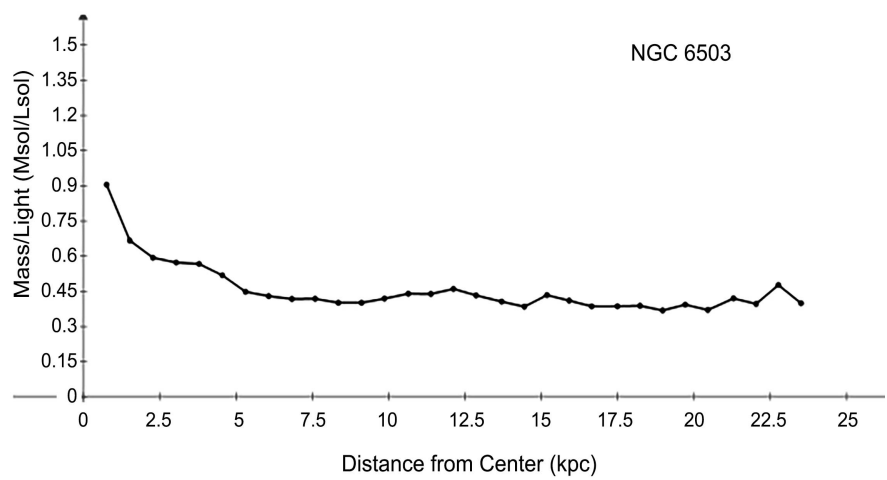
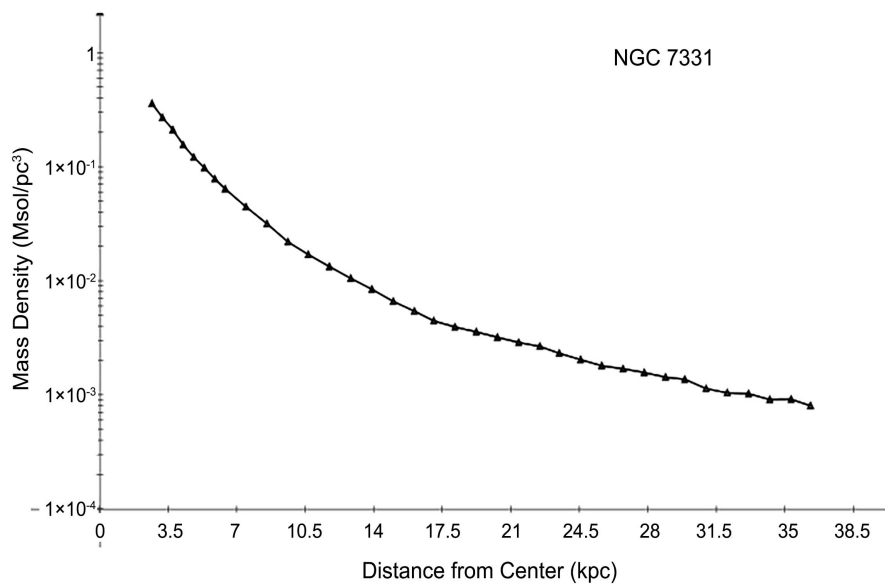
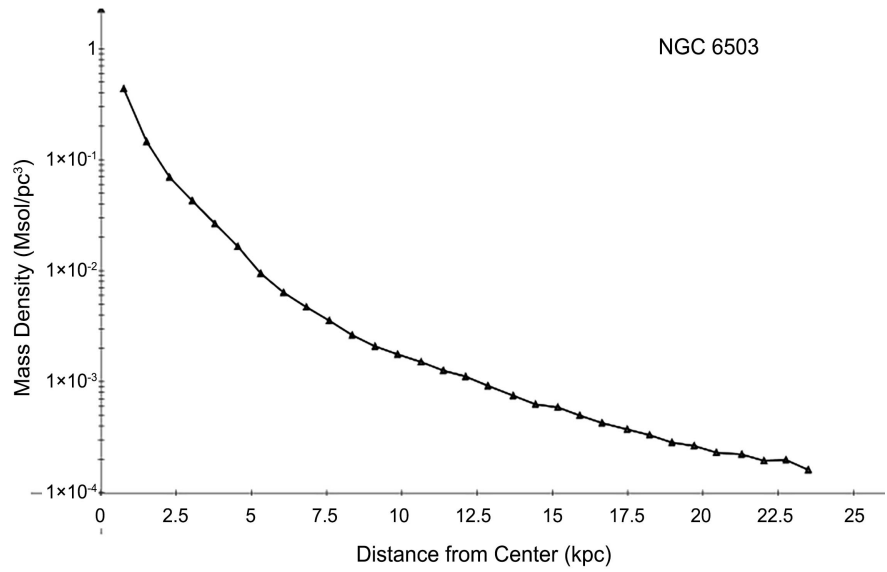


Figure A1. Fits with SPARC data, the mass density derived from (26) with velocity profiles for gas, disk and bulge. For mass to light curves, Υ_{disk} is the solid line and filled circles. For rotation velocity curves, the solid line is the minimised fit to the data with the graviton model (27) and the dashed line is the Newtonian velocity. Upper left: NGC 2903 mass density. Middle left: Mass to light ratio. Lower left: The model velocity vs. radial distance from the galactic center and the Newtonian velocity. Upper right: NGC 3198 mass density. Middle right: Mass to light ratio. Lower right: The model velocity vs. radial distance from the galactic center and the Newtonian velocity.



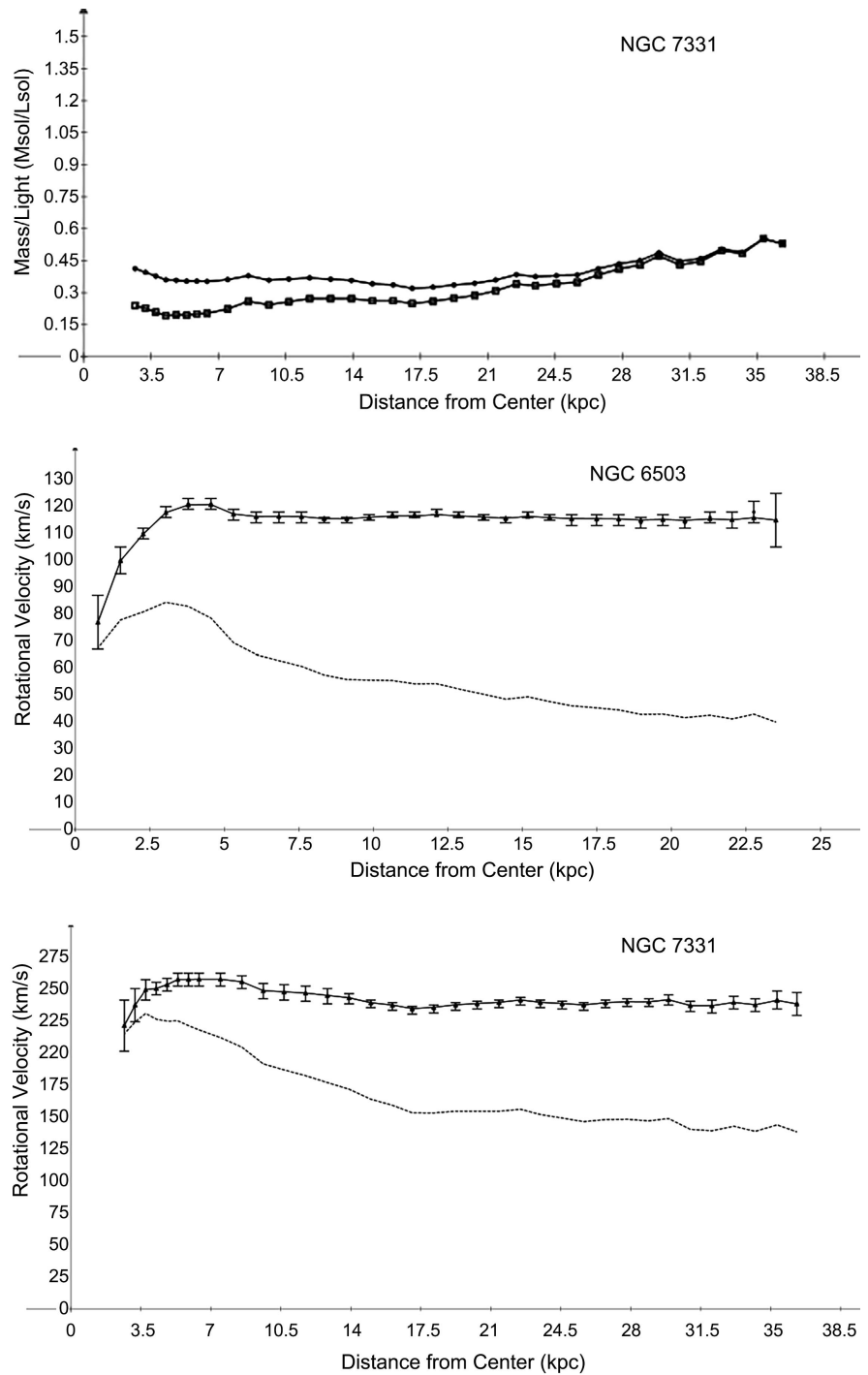
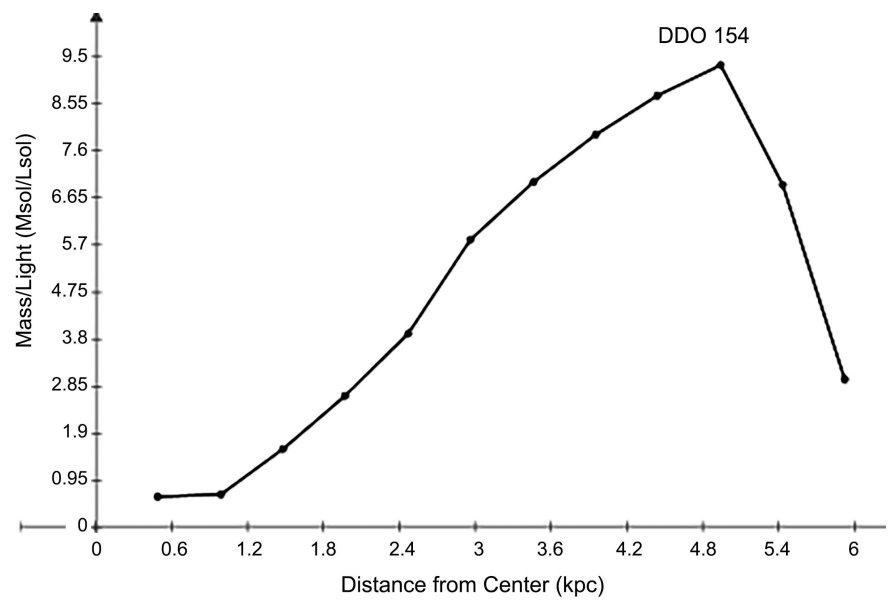
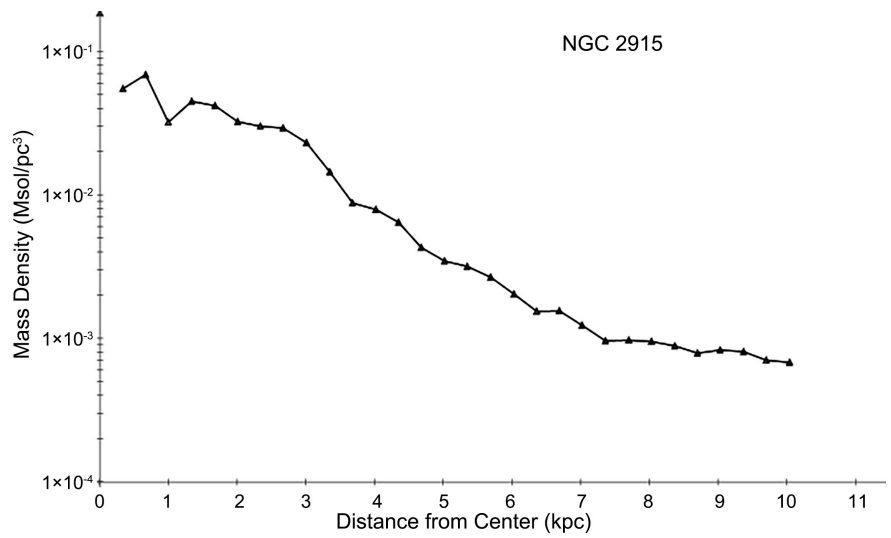
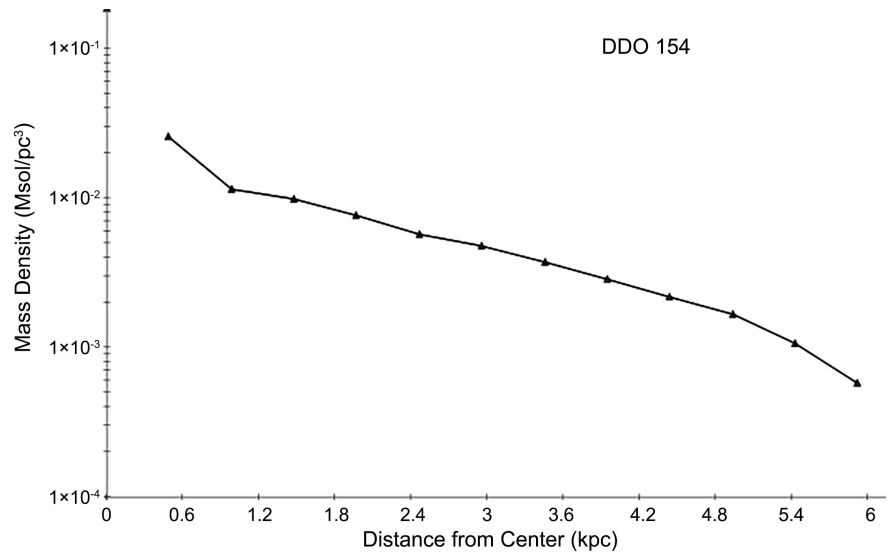


Figure A2. Fits with SPARC data, the mass density derived from (26) with velocity profiles for gas, disk and bulge. For mass to light curves, Υ_{disk} is the solid line and filled circles, Υ_{bul} is the solid line and open squares. For rotation velocity curves, the solid line is the minimised fit to the data with the graviton model (27) and the dashed line is the Newtonian velocity. Upper left: NGC 6503 mass density. Middle left: Mass to light ratio. Lower left: The model velocity vs. radial distance from the galactic center and the Newtonian velocity. Upper right: NGC 7331 mass density. Middle right: Mass to light ratio. Lower right: The model velocity vs. radial distance from the galactic center and the Newtonian velocity.



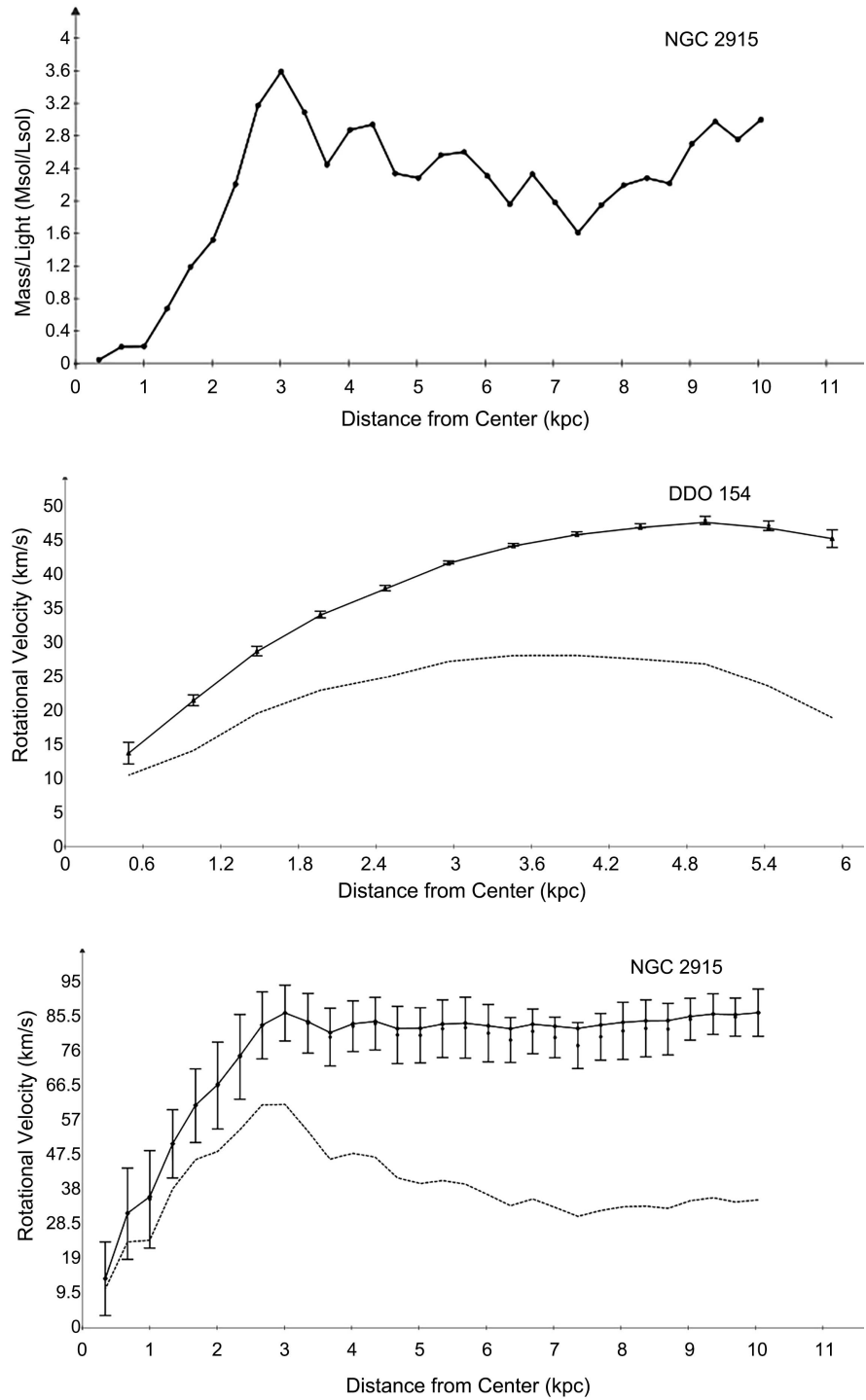
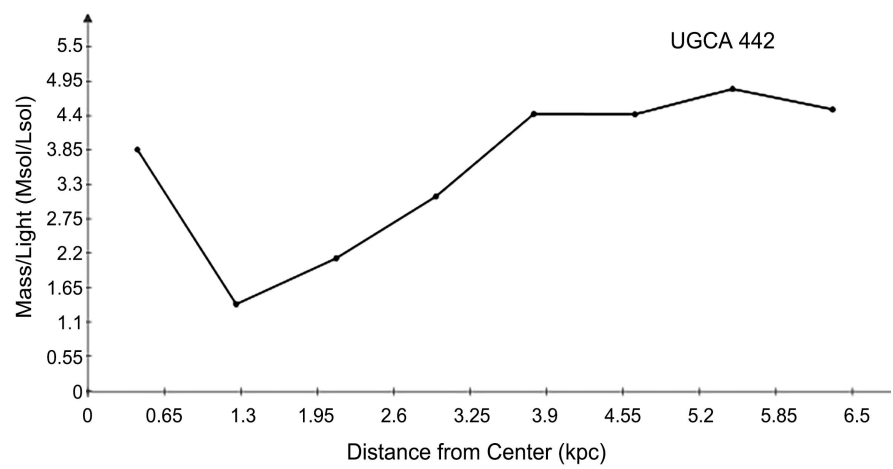
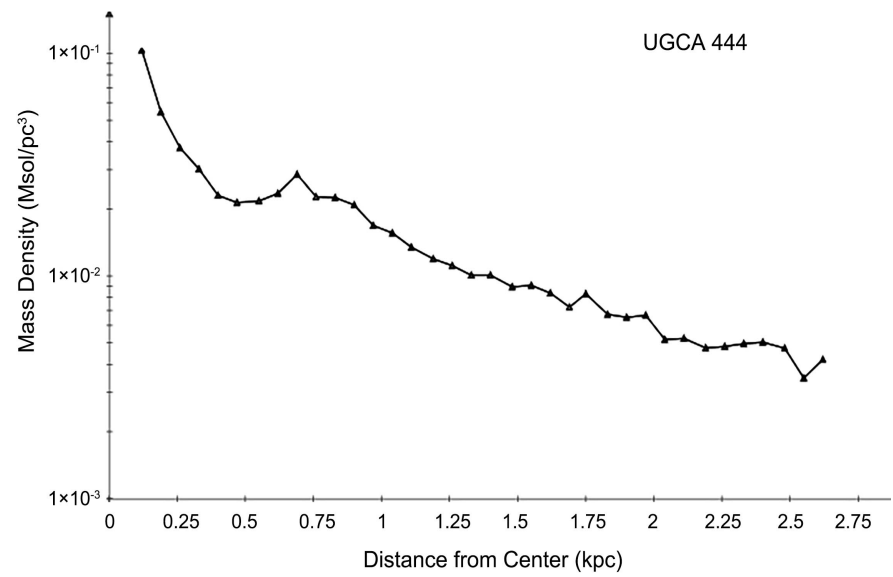
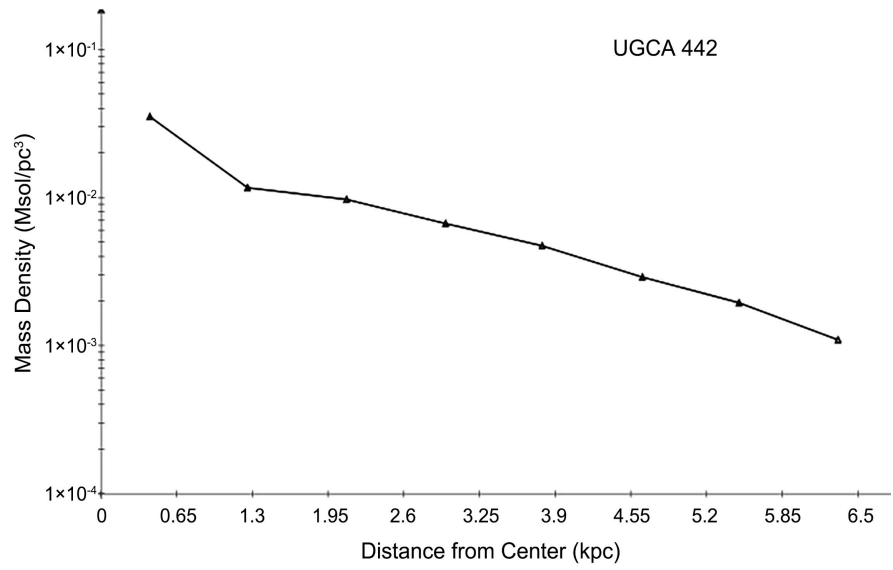


Figure A3. Fits with SPARC data, the mass density derived from (26) with velocity profiles for gas, disk and bulge. For mass to light curves, Υ_{disk} is the solid line and filled circles. For rotation velocity curves, the solid line is the minimised fit to the data with the graviton model (27) and the dashed line is the Newtonian velocity. Upper left: DDO 154 mass density. Middle left: Mass to light ratio. Lower left: The model velocity vs. radial distance from the galactic center and the Newtonian velocity. Upper right: NGC 2915 mass density. Middle right: Mass to light ratio. Lower right: The model velocity vs. radial distance from the galactic center and the Newtonian velocity.



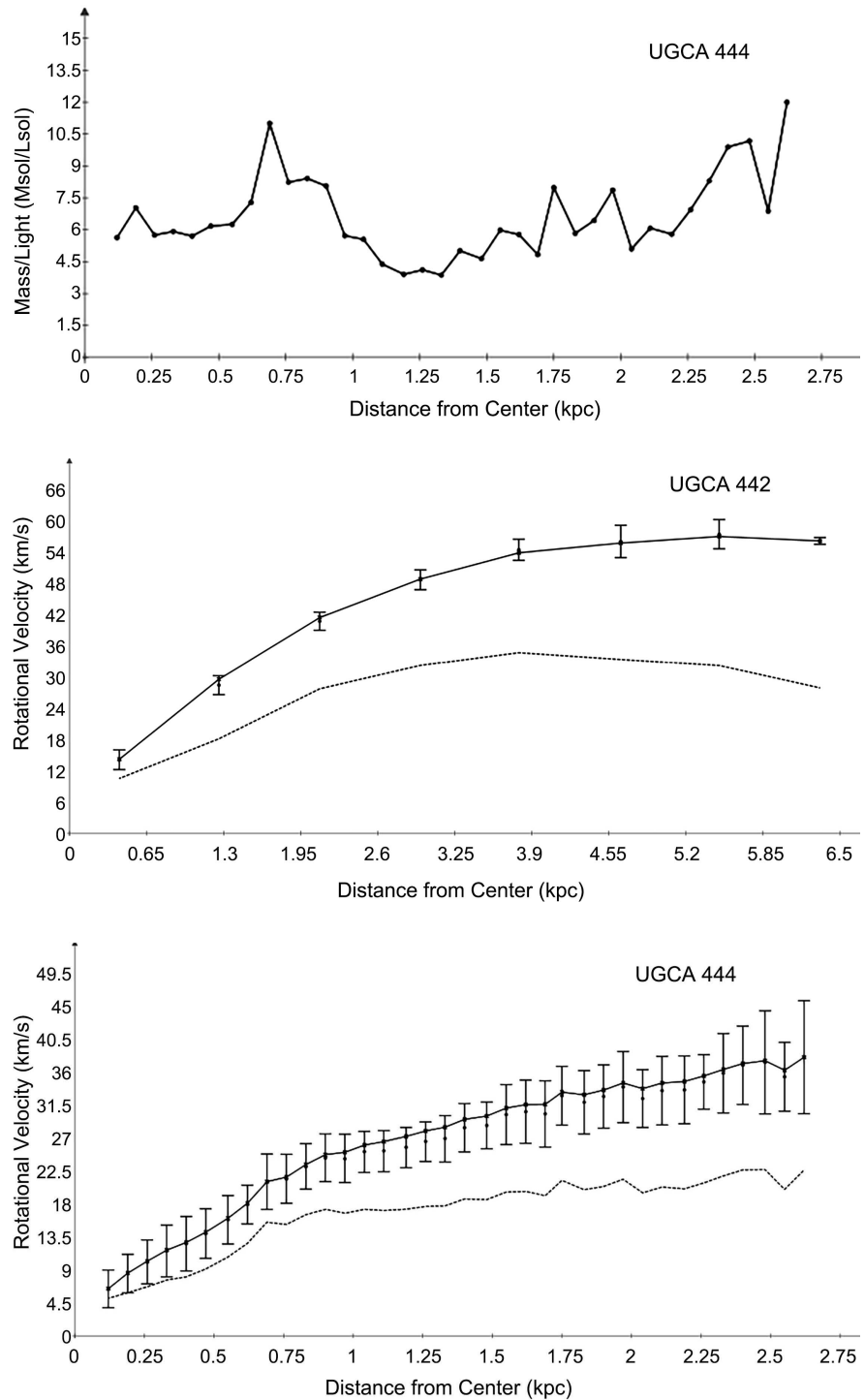
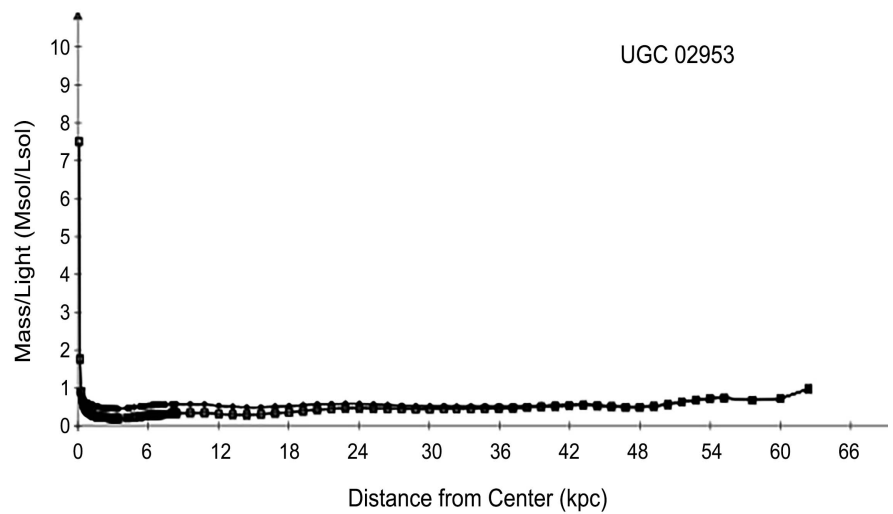
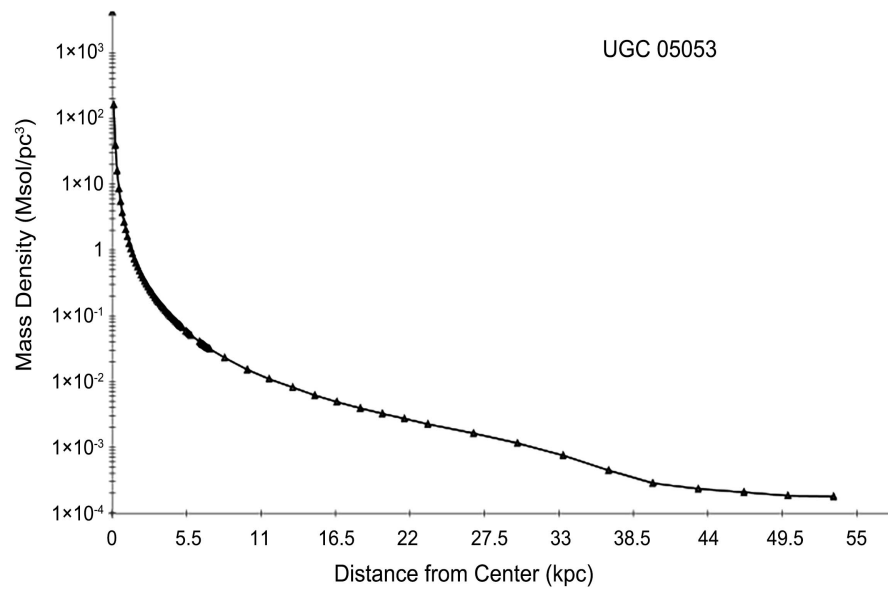
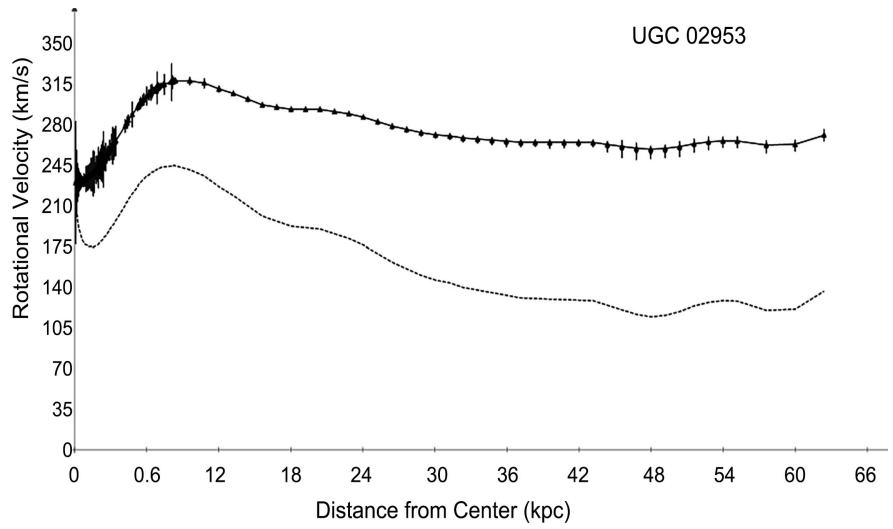


Figure A4. Fits with SPARC data, the mass density derived from (26) with velocity profiles for gas, disk and bulge. For mass to light curves, Υ_{disk} is the solid line and filled circles. For rotation velocity curves, the solid line is the minimised fit to the data with the graviton model (27) and the dashed line is the Newtonian velocity. Upper left: UGCA 442 mass density. Middle left: Mass to light ratio. Lower left: The model velocity vs. radial distance from the galactic center and the Newtonian velocity. Upper right: UGCA 444 mass density. Middle right: Mass to light ratio. Lower right: The model velocity vs. radial distance from the galactic center and the Newtonian velocity.



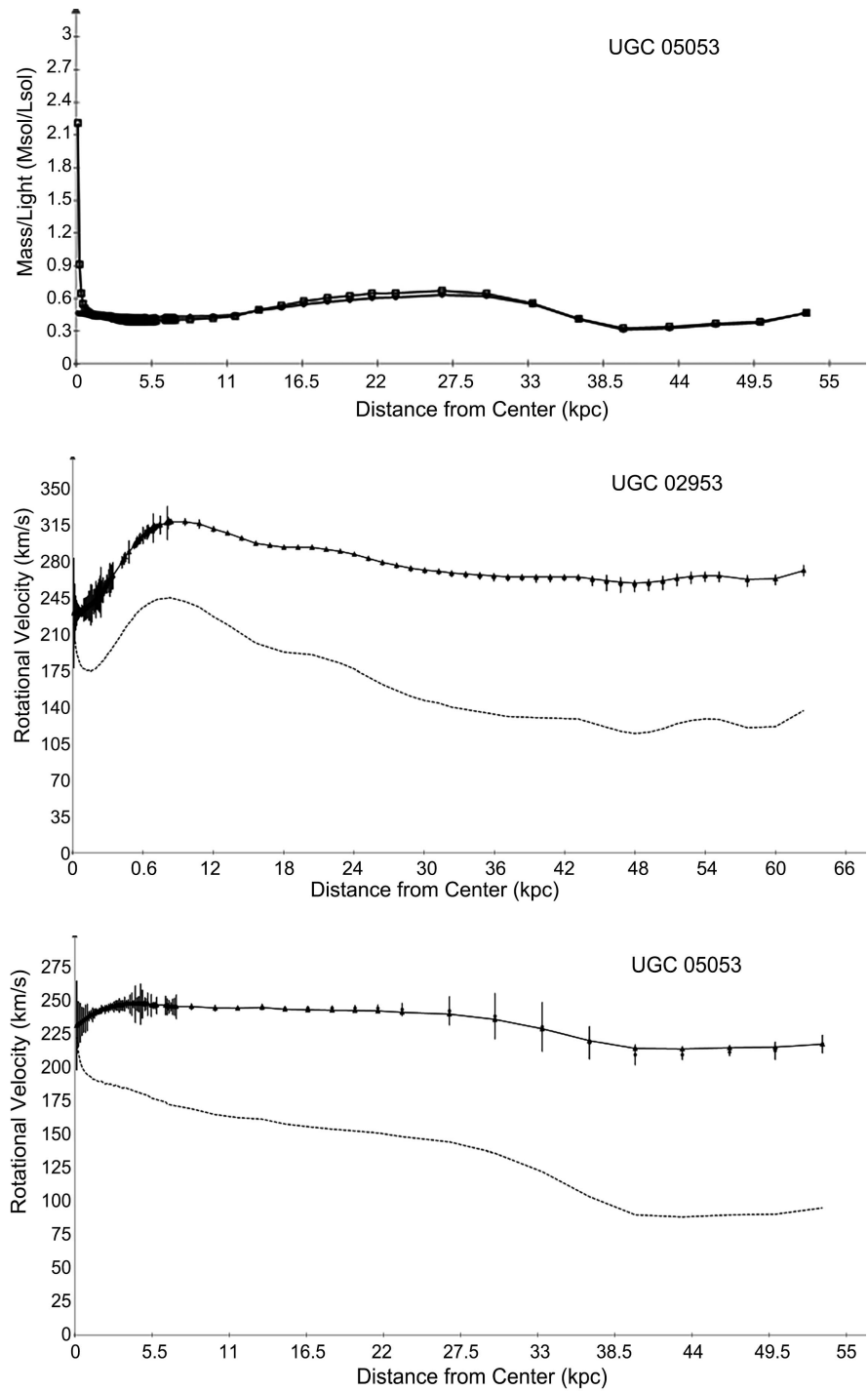
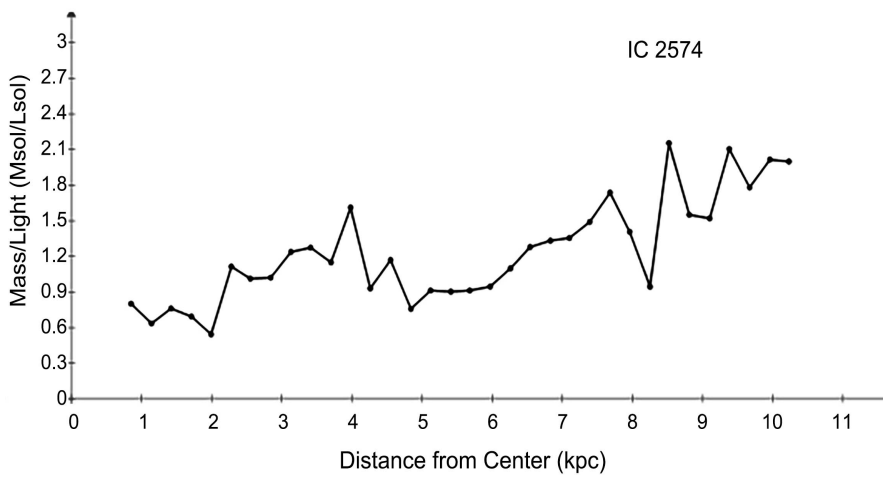
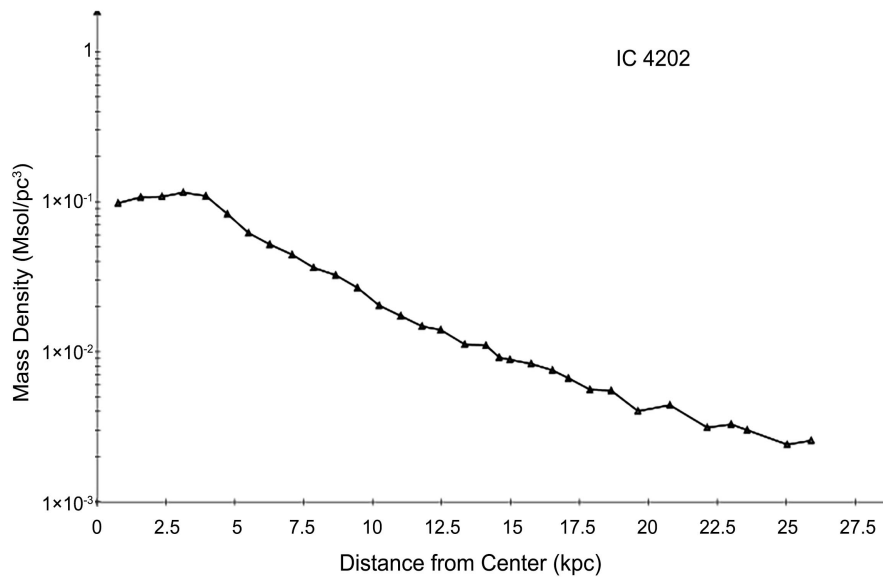
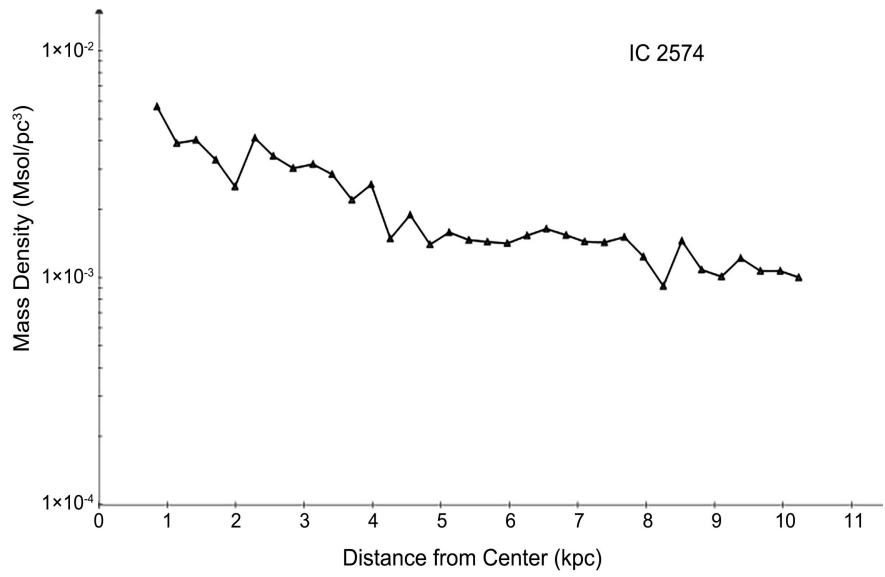


Figure A5. Fits with SPARC data, the mass density derived from (26) with velocity profiles for gas, disk and bulge. For mass to light curves, Υ_{disk} is the solid line and filled circles, Υ_{bul} is the solid line and open squares. For rotation velocity curves, the solid line is the minimised fit to the data with the graviton model (27) and the dashed line is the Newtonian velocity. Upper left: UGC 02953 mass density. Middle left: Mass to light ratio. Lower left: The model velocity vs. radial distance from the galactic center and the Newtonian velocity. Upper right: UGC 05053 mass density. Middle right: Mass to light ratio. Lower right: The model velocity vs. radial distance from the galactic center and the Newtonian velocity.



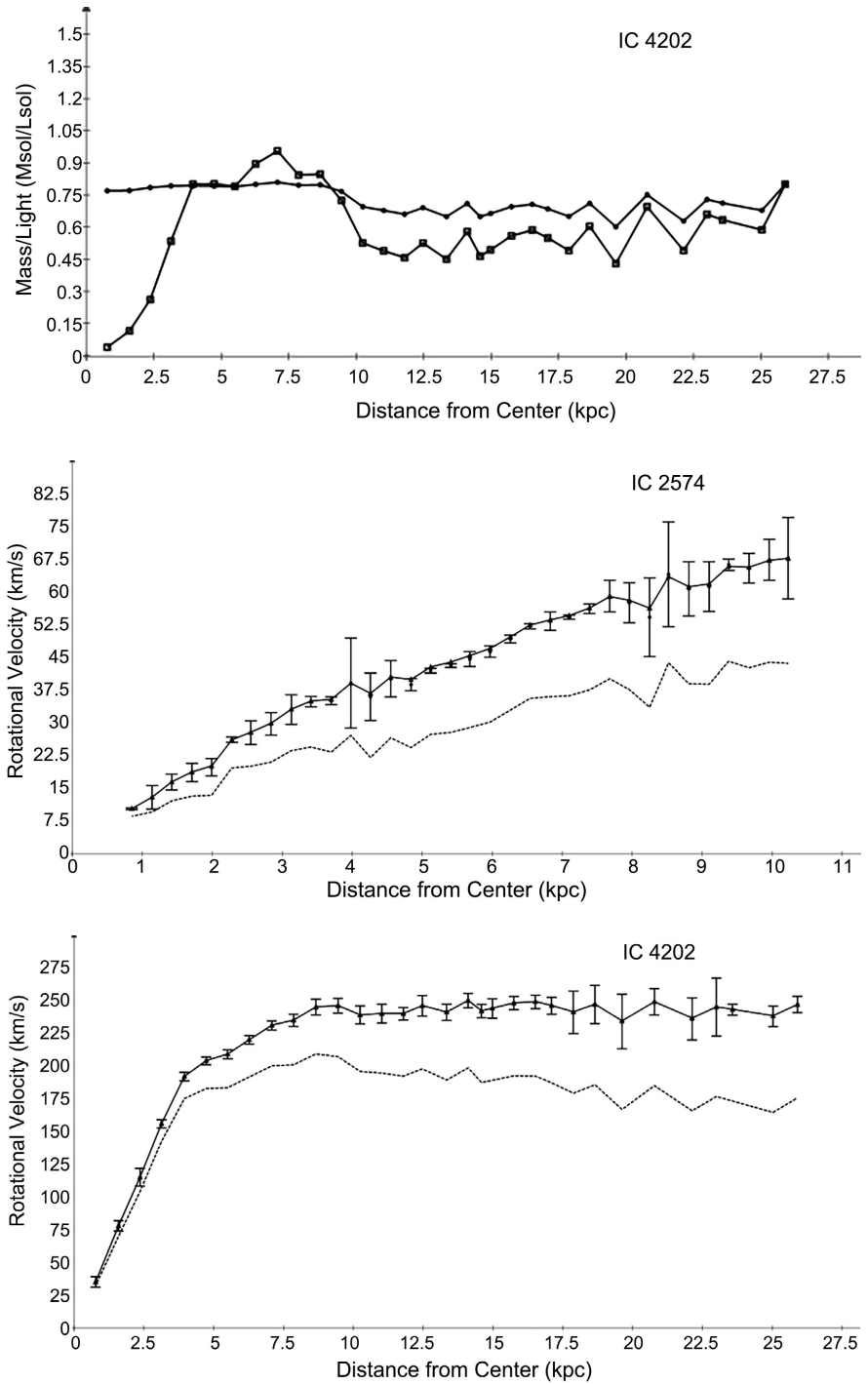


Figure A6. Fits with SPARC data, the mass density derived from (26) with velocity profiles for gas, disk and bulge. For mass to light curves, Υ_{disk} is the solid line and filled circles, Υ_{bul} is the solid line and open squares. For rotation velocity curves, the solid line is the minimised fit to the data with the graviton model (27) and the dashed line is the Newtonian velocity. Upper left: IC 2574 mass density. Middle left: Mass to light ratio. Lower left: The model velocity vs. radial distance from the galactic center and the Newtonian velocity. Upper right: IC 4202 mass density. Middle right: Mass to light ratio. Lower right: The model velocity vs. radial distance from the galactic center and the Newtonian velocity.